

An Improved Segmentation Algorithm For X-Ray Images Based On Adaptive Thresholding Classification

Anil K. Bharodiya, Atul M. Gonsai

Abstract: Medical image processing is a versatile human disease diagnoses system using MRI images, X-Ray images, Mammography, Ultra Sound, CT images etc. X-Ray imaging is a faster, cheaper, convenient and handy mechanism to detect bone-related diseases to support orthopaedics doctors or physicians. In medical image processing, once the X-Ray image is captured, it is fed to diseases diagnose system. This system does the task of image processing using specified processes. Segmentation is one of the processes of image classification in which an image under analysis is divided into its constituent sub-images. The accuracy of X-Ray image diagnoses is highly dependent on the segmentation process and hence, it is crucial for further image analysis. Many researchers have worked on image segmentation but the performance is subjective to the type of body image under diagnoses. In this research paper, we have proposed an improved algorithm, which is called adaptive thresholding classification (ATC) segmentation for human being's X-Ray image segmentation based on Gaussian filter and adaptive thresholding classification technique. The achieved accuracy and precision of this algorithm are 98.014% and 95.122% respectively. We have also presented a comprehensive comparison of our proposed algorithm with five existing latest methods/algorithms of medical image segmentation. Further, we have found that our proposed method is superior in terms of accuracy, specificity, precision, sensitivity/recall and F-score for human being's X-Ray image segmentation.

Index Terms: Adaptive, F-Score, Image Processing, Orthopaedics, Thresholding, Segmentation, Specificity, X-Ray.

1. INTRODUCTION

Medical image analysis is one of the evolving and innovative areas to enhance the accuracy of diseases diagnose and to provide better treatment to the patient. The ultimate goal of Computer Aided Diseases Diagnoses (CADD) system is to diagnose diseases from medical images in digital form [1]. CADD system accepts medical images and generates diseases analysis report to help medical practitioners in their decisions and better patient treatment. Images can be MRI, CT, X-Ray, Mammography, Ultra Sound, Cardiograph etc. X-Ray image is prescribed by orthopaedics doctor to diagnose bone related issues such as fracture, osteoporosis, bone infection, bone tumour, arthritis etc. X-Ray image processing includes many steps such as image acquisition, enhancement, edge detection, segmentation, ROI detection, interpretation etc. Out of which image segmentation is one of the classification process, which does the task of dividing the X-Ray image into its constituent sub-parts to detect region of interest. General medical image segmentation methods can be categorized into the following classes: classical image segmentation methods (thresholding, regions-based, and edges-based), pattern recognition-based, deformable models, wavelets-based methods, and atlas-based techniques [2]-[6]. Paper [6] describes various methods as follows. Thresholding is one of the most simple segmentation techniques. The disadvantage of thresholding methods is that they can be applied to a single-band image, such as a gray-scale image or a single band of a multi-band image. Region based methods have shown to be very useful and efficient segmentation techniques in image processing. However they have over-segmentation tendency, require manual initialization and are sensitive to noise. Clustering technique can be used for multi-

band images, but the number of groups must be established first. Classification-based algorithm requires a training phase. Deformable models are less sensitive to noise than the other techniques presented in this chapter, which make them suitable for complex medical image segmentation problems. Atlas-based methods use prior knowledge in order to perform segmentation, but they are time-consuming. Generally, thresholding, edge-based, region based, and classification-based algorithms can solve simple medical image segmentation problems. For complex medical images, which cannot be handled robustly by general segmentation methods, deformable models and atlas-based segmentation methods are the most appropriate. Another solution is to combine two or more segmentation techniques. As future work, we intend to combine a classical image segmentation technique for an initial segmentation and then to apply a deformable model in order to increase the segmentation accuracy. Bio-inspired algorithms are among the most powerful algorithms used for optimization. Recently, BIAs have proven efficiency in handling computationally complex problems. So, another idea is to use a bio-inspired optimization technique, for example to determine the input parameters, before applying a classical segmentation algorithm. The image segmentation is based on measurements taken from the image such as brightness, color, depth, pixel value in gray scale, texture. However, they have concluded that segmentation method selection is highly subjective on type of image under analysis [7]. Most of the image segmentation techniques found in the literature are for binary or gray image; however, there are very few segmentation threshold techniques on color images. In this subsection we show the basic threshold techniques: Global threshold, adaptive threshold, Otsu method and the most important research in this field [7]. Radiography is the photographic record of an image produced by the passage of an X-ray source through an object [8]. The following figures 1(a) and 1(b) depicts X-Ray images of human arm and left hand respectively.

- Anil K. Bharodiya, *BCA Department, UCCC & SPBCBA & SDHG College of BCA & I.T., Udhna, Surat - 394210, Gujarat, INDIA. Email: anilbharodiya@gmail.com (Correspondence Author)*
- Atul M. Gonsai, *Department of Computer Science, Saurashtra University, Rajkot- 360005, Gujarat, INDIA. Email: atul.gonsai@gmail.com*



Fig. 1. X-Ray image of human. (a) arm (b) Hand

In this paper, we have proposed an improved segmentation algorithm for X-Ray images based on adaptive thresholding classification and Gaussian filter. We have also shown that the proposed algorithm also performs segmentation much effectively on other types of standard image dataset. Further, we have also presented a comprehensive comparison of our proposed method with five existing latest methods/algorithms of image segmentation based on accuracy, specificity, precision, sensitivity/recall and F-score parameters. The paper is organized as follows: Section 2 discusses related work on latest image segmentation methods/algorithms. Section 3 describes methodology of segmentation of X-Ray images which includes background of thresholding and adaptive thresholding, flowchart of proposed algorithm and discussion on comparison metrics. Section 4 describes series of steps and pseudocode of an improved segmentation algorithm. In Section 5, we have conducted experiments in terms of comparison and discussed experimental results. Finally, the paper is concluded in Section 6 with future attempts to be made.

2 RELATED WORK

In Medical Decision Support System (MDSS), an X-Ray image analysis is a sophisticated process in which an X-Ray image of human body is passed as an input and it generates output to support decision of medical practitioners. Many researchers have shown their interest in segmentation of biomedical images. If edge detection and segmentation are performed accurately and precisely, further processing on X-Ray image becomes much easier to generate interpretation reports. Following paragraphs discuss about biomedical image segmentation related work of some latest methods/algorithms. Authors of paper [9] have presented a novel segmentation technique based on MsGKFCM clustering which automatically segments the breast US (ultra sound) images. This method achieves Accuracy (Mean±STD) 97.3158 ± 0.0409 , F-score (Mean±STD) 92.310 ± 0.0246 , Specificity (Mean±STD) 12.7777 ± 0.0246 , Precision (Mean±STD) 86.4956 ± 0.0244 , Recall (Mean±STD) 94.3291 ± 0.0385 . This method can be further improved by taking more than 90 image dataset. Researchers of paper [10] have proposed a novel region-growing segmentation method namely IPKD based on possibilistic theory on synthetic images as well as mammographic images from MIAS database. The advantage of this mechanism is to provide iterative diffusion of per-pixel certain knowledge to surrounding pixels in order to progressively refine the segmentation process. IPKD's performance (in terms of recognition rate, 94.37% and global predictive rate, 92.18%) is compared with three relevant reference methods: level-set, Fuzzy C-Mean and region growing methods. The IPKD approach outperforms the other three methods, respectively, at the recognition rates of

89.77%, 84.43% and 88.11% and at the global predictive rates of 87.86%, 89.72% and 84.04%. Gil Silva et al. [11] have presented a comprehensive comparative study of various segmentation techniques of dental X-Ray image such as Region growing, Splitting/merging, Global thresholding, Niblack method, Fuzzy C-means, Canny, Sobel Without edges, Level set method and Watershed. The maximum accuracy is 0.8234 in Fuzzy C-means, the maximum Specificity and Precision are 0.9958 and 0.8156 in Splitting/merging respectively, and the maximum recall and F-Score are 0.8257 and 0.6138 in Niblack method respectively. They have also presented a preliminary application of the MASK recurrent convolutional neural network to demonstrate the power of a deep learning method to segment images. Mahu and Minakshi [12] have demonstrated a comparative analysis of two binarization techniques- Niblack and Sauvola algorithm in context with their applications to retinal vessel segmentation. The result is compared with the ground truth images of DRIVE database. The method achieves 93.23% accuracy in case of Niblack's algorithm application and 93.31% (without post processing) and 94.34% (with post processing) accuracy in case of modified Sauvola binarization algorithm. Authors of paper [13] have proposed a deep learning based fully automatic a novel shape-aware framework for segmentation of cervical vertebrae in X-ray images. A Dice similarity coefficient of 0.84 and a shape error of 1.69 mm have been achieved. The shape-aware segmentation framework can further be improved to determine if a segmented vertebrae shape is regular or injurious/fractured. In the paper [14], authors have presented a novel convolutional neural network based deep learning approach for accurate segmentation of the sub-cortical brain structures that combines both convolutional and prior spatial features for improving the segmentation accuracy. DSC and HD of this algorithm were 0.843 and 4.493, respectively. Paper [15] has proposed a segmentation approach to integrate segmentations from region-based and boundary-based methods to tackle these typical segmentation problems. This approach can be further improved in terms of execution time and dice coefficient. Nguyen et al. [16] have developed a novel model based Super pixel and multi-atlas based fusion entropic for segmentation of X-Ray images of pelvis, talus and patella. Accuracy of Vol based fusion are 93.79% (Patella), 88.3% (Talus) and 85.02% (Pelvis), whereas, accuracy of SBA based fusion are 93.79% (Patella), 88.38% (Talus) and 85.01% (Pelvis). Authors of paper [17] have also worked on super pixel based Classification to devise a method for fully automatic multi-parametric segmentation of brain tumor in MR images. The algorithm achieved dice score of 91% to segment tumor in MR brain images using BRATS2012 dataset. It is difficult to locate tumor in the poor illumination conditions. Shen D. et al. [18] have proposed a robust and efficient learning-based deformable model for segmenting regions of interest (ROIs) from structural MR brain images. The achieved accuracy were 0.793, 0.811 and 0.854 in IXI, LONI and SATA dataset, respectively whereas, average time for segmentation is 5 minutes. This model can be further improved in terms of shape constraints, identification of more brain regions and exploring the DVM prediction. Authors of paper [19] have proposed a new semi-automatic multi-phase image segmentation algorithm that allows estimation of sub-resolution porosity for mono-mineral rocks. The algorithm is divided into three steps. First, purely solid and pure void

phases are segmented by a variant of hysteresis segmentation [20]. The residual phase is segmented with a statistical method in a number of distinct phases. Finally, expected porosity is calculated for each phase. Chen J. et al. [21] have proposed a novel image segmentation method based on fast density clustering algorithm (IS-FDC). Pixel similarity is calculated on basis of both pixel value and its position information. The accuracies of segmentation are 0.765, 0.581 and 0.571 in Poisson noises, Salt and Pepper noises and Gaussian noises, respectively. The paper is lacking in segmentation of high quality and complex images. Paper [22] used the LIDC-IDRI dataset with nodules of varied characteristics of lesions located in different regions of the lungs to evaluate the new developed methodology of nodule segmentation and volume measurement schemes. The average Dice scores are 82.35% and 71.05% for the two datasets. Ali and Hassan [23] have presented a novel method as MVGC for medical image segmentation based on mean value guided contour. In this method, the gradient vectors of edge map should be toward the edges so that it makes them almost parallel with the normal of edges, and have the magnitudes proportional to the edge saliency near them. The error rate of proposed method is 4.53% which is very low as compared to other methods such as InvComp9, InvComp3, Gauss-Newton, Classical etc. Further, this method can be extended to real 3D image classification. Chen. Y.T. [24] has proposed a novel approach for segmentation and visualization plus value-added surface area and volume measurements for brain medical image analysis. The execution time of algorithm is very low as compared to Chan-Vese model and GAC model. Authors of paper [25] have devised a new algorithm based on discrete step for X-Ray bone image segmentation. This paper opens improvements in Watershed Segmentation and Otsu's Segmentation. Paper [26] proposed a single universal network that can perform two tasks. First, segment different organs across different modalities, and Second, solve both segmentation and classification problems simultaneously. Dice score of this method can be further improved from 0.89 and segmentation of more organs and disease classification. Saidy and Lee [27] have presented a deep learning method of segmenting lungs in chest X-Ray image using Encoder-Decoder Convolutional Network on the JSRT (Japanese Society of Radiological Technology) lung nodule dataset. The achieved DSC, Sensitivity, Specificity and H. Distance are 0.962, 0.960, 0.992 and 3.889 respectively in Right Lungs. It is cleared from the above presented extensive literature review, that no method is perfect and suitable for all types of images. A particular segmentation method is subjective in nature because selection of method is highly dependent on type of image to be processed. It gives us relentlessly motivation to work in the field of segmentation of human X-Ray image and here, in this paper we have presented an improved segmentation algorithm called ATC segmentation for X-Ray images based on adaptive thresholding classification.

3 METHODOLOGY

In this section, we have discussed methodology of proposed method for segmentation. We have divided it into three sub-sections such as adaptive thresholding segmentation, evaluation metrics used for comparison and flow chart of an improved segmentation algorithm.

3.1 Adaptive Thresholding

Thresholding is an image segmentation method in which one threshold value is decided. This value can be standard or mean of pixel values of an image. If the pixel value is greater than threshold value then, that pixel is considered in foreground. Similarly if the value is less than the threshold value then, that pixel or part appears in the background. In the case of adaptive thresholding, the threshold value changes dynamically over the image based on the contrast, texture, resolution, types etc. of an image [28]. There are many methods to decide optimal threshold value such as Otsu's Method, Kapur's method, Rosin's method, Entropy method etc. We have decided threshold values based on combining two approaches such as fixed grayscale pixel values of an X-Ray image of human arm through experiments and pixel values obtained from Otsu's Method [29].

3.2 Evaluation Metrics

Metrics are performance evaluators for any method or algorithm. In this paper, we have considered different metrics of binary classification to measure the performance of our ATC segmentation method. Tables 1 and 2 depict initial measures and performance measures of different image segmentation algorithms respectively [11].

TABLE I: INITIAL MEASURE.

| Measure | Description |
|---------------------|---|
| Positive (P) | Pixel is in a class of interest. |
| Negative (N) | Pixel is not in a class of interest. |
| True Positive (TP) | The pixel in the ground truth is positive, while method ranks the pixel as positive. <u>For Example:</u> pixels correctly labelled as tumor. |
| True Negative (TN) | The pixel in the ground truth is negative, while method ranks the pixel as negative. <u>For Example:</u> pixels correctly labelled as healthy tissue. |
| False Positive (FP) | The pixel in the ground truth is negative, while method ranks as positive. <u>For Example:</u> pixels wrongly labelled as tumor. |
| False Negative (FN) | The pixel in the ground truth is positive, while method ranks the pixel as negative. <u>For Example:</u> pixels wrongly labelled as healthy tissue. |

TABLE II: METRICS USED FOR PERFORMANCE EVALUATION

| Measure | Description |
|---------------------|--|
| Accuracy | Relation between total of hits on the total set of errors and hits. This value is calculated by: $(TP + TN)/(TP + FN + FP + TN)$ |
| Specificity | Percentage of negative samples correctly identified on total negative samples. This value is calculated by: $TN/(FP + TN)$ |
| Precision | Percentage of positive samples correctly classified on the total of samples classified as positive. This value is calculated by: $TP/(TP + FP)$ |
| Sensitivity/ Recall | Percentage of positive samples correctly classified on the total of positive samples. This value is calculated by: $TP/(TP + FN)$ |
| F-score | Represents the harmonic average between precision and sensitivity. It is calculated by: $2 * Recall * Precision / (Recall + Precision)$ |
| FDR | The FDR is the rate that features called significant are truly null. $FDR = FP / (FP + TP) = 1 - PPV$ (PPV means Positive Predictive Value or Precision) |
| Fall-out / FPR | The FPR or per comparison error rate (PCER) is the rate at which the number of events wrongly categorized as positive (false positive) but in reality it is negative. FP is one type of error. $FPR = FP / N = FP / (FP + TN) = 1 - TNR$ (TNR means True Negative Rate or Specificity) |

| | |
|-----------------|---|
| Miss Rate / FNR | The FNR is the rate at which number of events wrongly categorized as negative (false negative) but in reality it is positive. FN is one type of error. $FNR=FN/(FN+TP)=1-TPR$ (TPR means True Positive Rate or Sensitivity) |
|-----------------|---|

3.3 Flowchart

Fig. 2 represents the complete flowchart of proposed ATC segmentation algorithm for human X-Ray images. This algorithm accepts an X-Ray image as an input and if it is RGB/24bits then, we have converted into grayscale image. Image may contain noise, improper blurring or out of focus that is why we have pre-processed it. We have applied 2D Gaussian filter to blur X-Ray image and remove detail and noise. Gaussian filter is similar to the mean filter which is used to remove both types noises Gaussian and salt & pepper. It helps to detect false edges due to noise. As per paper [30] the Gaussian filter is depends on two principles. First, the joint conditional predictive state is assumed to be a Gaussian Probability Distribution Function for linear structure and second, for nonlinear functions there should be models to be approximated. The formula for 2D Gaussian filter is given below [31].

$$G(X, Y) = \frac{1}{2\pi\sigma^2} \cdot e^{-\frac{x^2+y^2}{2\sigma^2}} \quad (1)$$

Where, x is the distance from the origin in the horizontal axis, y is the distance from the origin in the vertical axis, and σ is the standard deviation of the Gaussian distribution. In the next stage, adaptive thresholding classification is applied which distribute every pixel of processed X-Ray image into three classes say Black, Gray and white or Background Part, Tissue/Skin part and bony part respectively. This classification is carried out on the basis of intensity values of the pixels of an X-Ray image. Further, the pixel values are converted into Scilab uint8 data type to display segmented image as output.

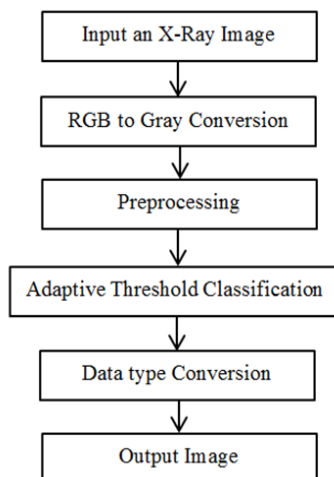


Fig. 2. Flowchart of the proposed method.

We have compared our proposed ATC Segmentation algorithm with five latest methods/algorithms such as MsGKFCM Technique [9], IPKD Approach [10], MASK R-CNN Method [11], Modified Sauvola's, Binarization [12] and Unet-S [13]. In comparative study, we have considered Accuracy, Specificity, Precision, Recall/Sensitivity, F-Score, FDR, FPR and FNR as

performance analysis parameters. We have shown that our algorithm is superior.

4 PROPOSED METHOD FOR X-RAY IMAGE SEGMENTATION

An algorithm is a sophisticated series of steps to be processed to arrive at a particular decision for solution of a problem. We have devised an ATC segmentation algorithm in following steps for segmentation of human X-Ray images.

Algorithm: Edge Detection from X-Ray Images

- Step-1 : Input an X-Ray Image.
- Step-2 : Perform rgb2gray to convert it in gray scale
- Step-3 : Gaussian filter.
- Step-4 : Divide an image into three classes. If pixel value is between 0 and 10 then, set pixel value 0 (mark as Black, It means background part), If pixel value is between 11 and 128 then, set pixel value 120 (mark as Gray, It means tissue or skin part), Else set pixel value 255 (mark as White, it means bony part).
- Step-5 : Convert an image of step-4 in uint8 data type to show as grayscale image. (for Scilab)
- Step-6 : Show an image of step-5 as output with Image Segmentation.

In step-1 image is inputted by the user. Step-2 converts an RGB X-Ray image into gray scale image. Step-3 does Gaussian filter. This filter blurs the image. Step-4 partitions an inputted image into 3 broad classes on the basis of pixel intensity. If pixel value is between 0 and 10 then, set pixel value 0 for that pixel (mark as Black, It means background part), If pixel value is between 11 and 128 then, set pixel value 120 for that pixel (mark as Gray, It means tissue or skin part), Else set pixel value 255 for that pixel (mar as White, it means bony part). In Step-5 we have done conversion of step-4 image into grayscale image by using uint8 data type of Scilab. Finally, Step-6 displays the output image with segmentation.

5 EXPERIMENTAL RESULT AND DISCUSSION

IJSTR This section presents the segmentation experiments of proposed ATC segmentation algorithm and comparative evaluation of different image segmentation methods/algorithms. To evaluate the performance of the proposed algorithm, experiments have been conducted and the results were compared with five latest image segmentation methods. The experiments were evaluated on 59 human X-Ray images, however, due to space limitation, the result of 5 images (Figs. 3) are shown in this paper to illustrate the effectiveness of proposed algorithm. Test images were collected from hospital in person, downloaded from google images, NHA and imageprocessingplace.com. Table – 3 shows computer system environment on which proposed ATC segmentation algorithm has been evaluated.

TABLE III: ENVIRONMENT OF MACHINE.

| Environment of Machine | |
|------------------------|----------------------------------|
| Operating System | Windows 7 SP 1 (64 bit) |
| Image Processing S/W. | Scilab 5.5.2 |
| Image Size | 512 * 512, 8 bit grayscale, .jpg |
| Processor | Intel Core i5 1.70 GHz |
| RAM | 4 GB |
| HDD Capacity | 500 GB |

Fig. 3 shows experiments of ATC segmentation algorithm on X-Ray images. It is clear from the Fig.3 that our algorithm is able to do segmentation not only for X-Ray images but also for

other standard images. The segmentation quality and accuracy of our algorithm is better in visualization and analysis. We have compared ATC segmentation algorithm with five latest image segmentation methods/algorithms such as Multi-scale Gaussian Kernel induced Fuzzy C-means (MsGKFCM) Technique [9], Iterative Possibilistic Knowledge Diffusion (IPKD) Approach [10], MASK recurrent convolutional neural network (MASK R-CNN) Method [11], Modified Sauvola's, Binarization [12] and Unity Network – Shape aware (Unet-S) method [13]. Section 3.2 gives a complete list of evaluation metrics that we have considered to compare the results of our ATC segmentation algorithm with these five methods. Table – 4 provides comparison of aforementioned five latest image segmentation methods/algorithms and our ATC segmentation algorithm based on metrics given in table – 2.

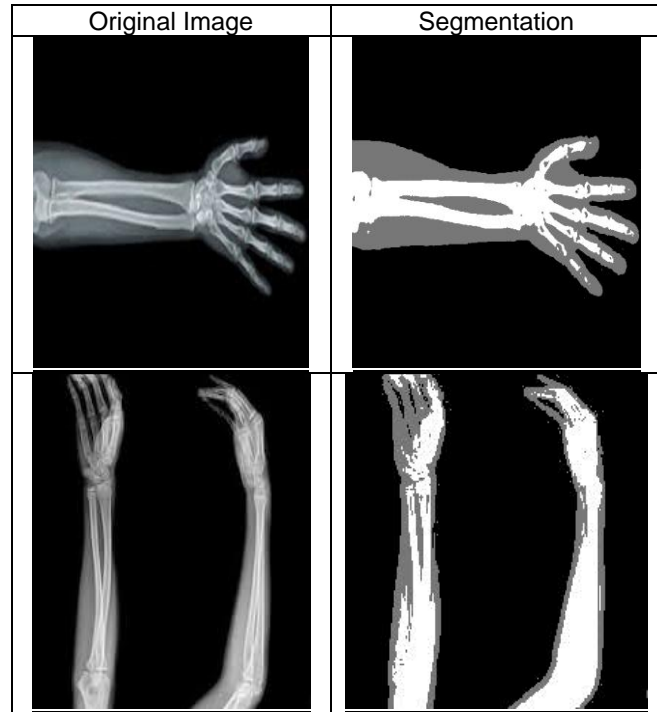


Fig. 3. Image segmentation using ATC segmentation algorithm

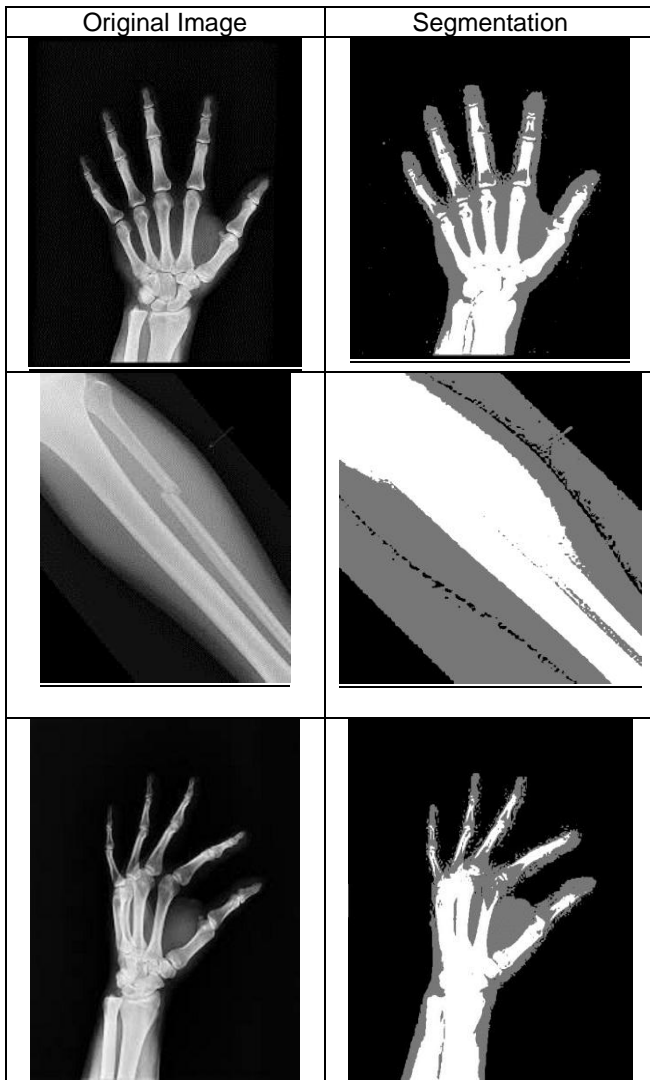


Table – 4 presents the performance of different segmentation techniques in terms of Accuracy, Specificity, Precision, Recall/ Sensitivity, F-Score, FDR, FPR and FNR. It is observed that the accuracy of proposed ATC segmentation algorithm is improved by 0.739%, 14.673%, 5.934%, 3.670% and 2.804% as compared to MsGKFCM, IPKD, MASK R-CNN, Modified Sauvola's Binarization and Unet-S methods respectively. Precision of ATC segmentation algorithm is improved by 8.651%, 15.873%, 11.392%, 16.357% and 6.012% as compared to MsGKFCM, IPKD, MASK R-CNN, Modified Sauvola's Binarization and Unet-S methods respectively. The average accuracy and precision of ATC segmentation method are 98.014%, 95.122% respectively, which are very high as compared to other five methods given in Table – 4. This algorithm achieved higher accuracy and precision due to combination of Gaussian filter, fixed grayscale pixel values and optimal threshold values obtained based on Ostu's method. The Specificity of ATC segmentation algorithm is improved by 78.267% and 9.861% as compared to MsGKFCM and IPKD respectively, while, it is decreased by 5.100%, 6.100% and 4.980% as compared MASK R-CNN, Modified Sauvola's Binarization and Unet-S methods respectively. It means our algorithm achieved more specificity as compared to two methods and less specificity as compared to three methods. The sensitivity/Recall rate of ATC segmentation algorithm is improved by 6.076%, 15.833%, 20.913% and 1.563% as compared to IPKD, MASK R-CNN, Modified Sauvola's Binarization and Unet-S methods respectively, while, it is decreased by 2.268% only as compared to MsGKFCM method. F-Score is a harmonic mean of Recall and Precision rate. It is improved in ATC segmentation algorithm by 3.383%, 11.133%, 14.155%, 18.853% and 1.293% as compared to MsGKFCM, IPKD, MASK R-CNN, Modified Sauvola's Binarization and Unet-S methods respectively. The higher rate of F-Score guarantees better segmentation because both metrics are based on correct positives. As per

above Table- 4, the proposed algorithm achieves higher F-Score. FDR, FPR and FNR are error metrics to show false segmentation. The less rate of these parameters guarantee better segmentation. The FDR of our proposed ATC segmentation algorithm is only 4.878% which is less than 13.529% (MsGKFCM), 20.751% (IPKD), 16.270% (MASK R-CNN), 21.235% (Modified Sauvola's Binarization) and 10.890% (Unet-S). The FPR is 8.980% which is less than 87.247% (MsGKFCM) and 18.841% (IPKD), while, it is greater than 3.880% (MASK R-CNN), 2.880% (Modified Sauvola's Binarization) and 4.000% (Unet-S). The FNR is 7.977% which is less than 14.053% (IPKD), 23.810% (MASK R-CNN), 28.890% (Modified Sauvola's Binarization) and 9.540% (Unet-S), while, it is greater than 5.709% (MsGKFCM). As per above interpretation derived from table – 4, it is cleared that our ATC segmentation algorithm does X-Ray image segmentation very efficiently and effectively as compared to MsGKFCM, IPKD, MASK R-CNN, Modified Sauvola's Binarization and Unet-S methods in terms of accuracy and precision. The error rates

say FDR, FPR and FNR are very low as compared to these five methods of image segmentation. The proposed segmentation algorithm is superior as compared to latest other five techniques or methods used for medical image segmentation as given in Table-4. The parameters of comparison such as Accuracy, Specificity, Precision, Recall/Sensitivity, F-Score, FDR, FPR and FNR are selected on the basis of latest research papers.

TABLE- IV: COMPARISON OF X-RAY IMAGE SEGMENTATION ALGORITHMS (VALUES ARE IN %)

| No. | Method Name | Accuracy | Specificity | Precision | Recall/ Sensitivity | F-Score | FDR | FPR | FNR |
|-----|--------------------------------------|----------|-------------|-----------|------------------------|---------|--------|--------|--------|
| 1 | MsGKFCM Technique [9] | 97.275 | 12.753 | 86.471 | 94.291 | 90.212 | 13.529 | 87.247 | 5.709 |
| 2 | IPKD Approach [10] | 83.341 | 81.159 | 79.249 | 85.947 | 82.462 | 20.751 | 18.841 | 14.053 |
| 3 | MASK R-CNN Method [11] | 92.080 | 96.120 | 83.730 | 76.190 | 79.440 | 16.270 | 3.880 | 23.810 |
| 4 | Modified Sauvola's Binarization [12] | 94.344 | 97.120 | 78.765 | 71.110 | 74.742 | 21.235 | 2.880 | 28.890 |
| 5 | Unet-S [13] | 95.210 | 96.00 | 89.110 | 90.460 | 92.302 | 10.890 | 4.000 | 9.540 |
| 6 | Proposed ATC Segmentation | 98.014 | 91.020 | 95.122 | 92.023 | 93.595 | 4.878 | 8.980 | 7.977 |

5 CONCLUSION AND FUTURE ATTEMPTS

In this paper, we have presented an improved algorithm namely ATC segmentation for segmentation of human's arm X-Ray images based on Gaussian filter and adaptive thresholding classification technique. This algorithm is able to do segmentation not only for X-Ray images but also for other standard images. We have considered Accuracy, Specificity, Precision, Recall/ Sensitivity, F-Score, FDR, FPR and FNR as performance evaluation metrics. We have also compared results of our ATC segmentation algorithm with five latest methods/algorithms. According to above Table – 4, proposed ATC segmentation algorithm achieved average results of 98.014% (accuracy), 91.020% (specificity), 95.122% (precision), 92.023% (recall) and 93.595% (F-score). The error rates say FDR (4.878%), FPR (8.980%) and FNR (7.977%) are very less as compared to other latest methods/algorithms. These values indicate that ATC segmentation algorithm achieved high number of true positives and true negatives, and low number of false positives and false negatives. It is cleared from Fig.3 and table – 4 that proposed ATC segmentation algorithm can do segmentation much better as compared to five latest methods such as MsGKFCM, IPKD, MASK R-CNN, Modified Sauvola's Binarization and Unet-S. The proposed algorithm can be used in medical field to develop CADD or DSS based on human X-Ray images or other types of digital images. Researcher can add more features, comparisons and parameters to further evolve and analyse proposed algorithm.

CONFLICT OF INTEREST

We, authors of this paper have equally contributed in research work. Further, we declare that there is no conflict of interest for this publication.

ACKNOWLEDGMENT

We thank Dr. Hemantbhai Patel of MGGZ Medical Centre, Surat, Gujarat, INDIA and Dr. Rajeshbhai Diyora of Madhav Orthopaedics, Surat, Gujarat, INDIA for their guidance related to X-Ray imaging and providing digital X-Ray images in soft copy.

REFERENCES

- [1] Bharodiya, A.K., Gonsai, A.M.: 'Research Review on feature extraction methods of human being's X-Ray image analysis', National Journal of System and Information Technology, 11(1), pp. 9-22, 2018.
- [2] Zharkova, V., Ipson, S., Abouardham, J., et al.: 'Survey of image processing techniques', EGSO internal deliverable, Report number EGSO-5-D1_F03-20021029, October, pp. 35-35, 2002 [Online]. Available: http://utopia.csis.pace.edu/dps/2007/amannettewright/dps/Software_Analysis/simulated_annealing_and_other_techniques.pdf
- [3] Feng, D.: 'Segmentation of Bone Structures in X-ray Image', PhD thesis, School of Computing National University of Singapore, under guidance of Dr. Leow Wee Kheng (Associate Professor), 2006. [Online]. Available: <http://www.comp.nus.edu.sg/~leowwk/thesis/dingfeng->

- proposal.pdf
- [4] Dougherty, G.: 'Medical Image Processing Techniques and Applications', Springer, 2011.
- [5] Russ, J. C.: 'Image Processing Handbook, the Sixth Edition', CRC Press Taylor & Francis Group, 2011.
- [6] Cristina, S.C., HOLBAN, S.: 'A Comparison of X-Ray Image Segmentation Techniques', *Advances in Electrical and Computer Engineering*, 2013, 13 (3), pp. 85-92
- [7] Lamont, F.G., Cervantes, J., Lopez, A., et al.: 'Segmentation of images by color features: A survey', *Neurocomputing*, 292, pp. 1-27, 2018.
- [8] Quinn, R. A., Sigl, C. C.: 'Radiography in Modern Industry, volume 4Th Edition', 1980.
- [9] Panigrahi, L., Verma, K., Singh, B.K.: 'Ultrasound Image Segmentation Using A Novel Multi-Scale Gaussian Kernel Fuzzy Clustering and Multi-Scale Vector Field Convolution', *Expert Systems With Applications*, pp.1-17, 2018.
- [10] Kallel, I.K., Almouahed, S., Solaiman, B., et al.: 'An Iterative Possibilistic Knowledge Diffusion Approach for Blind Medical Image Segmentation', *Pattern Recognition*, pp. 1-32, 2018.
- [11] Silva, G., Oliveira, L., Pithon, M. : 'Automatic segmenting teeth in X-ray images: Trends, a novel data set, benchmarking and future perspectives', *Expert Systems with Applications*, pp.1-38, 2018.
- [12] Nandy, M., Banerjee, M.: 'A Comparative Analysis of Application of Niblack and Sauvola Binarization to Retinal Vessel Segmentation', *IEEE International Conference on Computational Intelligence and Networks*, Bhubaneswar, Odisha, India, pp.105-109, 2017.
- [13] Arif, S.S., Knapp, K., Slabaugh, G., et al.: 'Fully automatic cervical vertebrae segmentation framework for X-ray images', *Computer Methods and Programs in Biomedicine*, 157, pp.1-41, 2018.
- [14] Kushibar, K., Valverde, S., Gonzalez-Villa, S., et al.: 'Automated sub-cortical brain structure segmentation combining spatial and deep convolutional features', *Medical Image Analysis* 48, pp. 177–186, 2018.
- [15] Su, L., Fu, X., Zhang, X., et al. : 'Delineation of carpal bones from hand X-ray images through prior model, and integration of region-based and boundary-based segmentations', *IEEE Access*, pp. 19993 – 20008, 2018.
- [16] Nguyen, D.C.T., Benameur, S., Mignotte, M., et al. ; 'Superpixel and multi-atlas based fusion entropic model for the segmentation of X-ray images', *Medical Image Analysis*, 48, pp. 58-74, 2018.
- [17] Rehman, Z. U., Naqvi, S.S., Khan, T.M., et al.: 'Fully Automated Multi-parametric Brain Tumour Segmentation using Superpixel based Classification', *Expert Systems with Applications*, 118, pp. 598-613, 2019.
- [18] Wu, Z., Guo, Y., Park, S.H., et al.: 'Robust Brain ROI Segmentation by Deformation Regression and Deformable Shape Model', *Medical Image Analysis*, 43, pp. 198-213, 2018.
- [19] Smal, P., Gouze, P., Rodriguez, O.: 'An automatic segmentation algorithm for retrieving sub-resolution porosity from X-ray tomography images', *Journal of Petroleum Science and Engineering*, 166, pp. 198-207, 2018.
- [20] Vera, S., Perez, F., Lara, L., et al.: 'A threshold with hysteresis', *The Insight Journal*, 2011.
- [21] Chen, J., Zheng, H., Lin, X., et al.: 'A novel image segmentation method based on fast density clustering algorithm', *Engineering Applications of Artificial Intelligence*, 73, pp.92–110, 2018.
- [22] Shakibapoura, E., Cunha, A., Aresta, G., et al.: 'An unsupervised metaheuristic search approach for segmentation and volume measurement of pulmonary nodules in lung CT scans', *Expert Systems with Applications*, 119, pp. 415-428, 2019.
- [23] Kiaei, A.A., Khotanlou, H.: 'Segmentation of Medical Images using Mean Value Guided Contour', *Medical Image Analysis*, 40, pp. 111-132, 2017.
- [24] Chen, Y.T.: 'A novel approach to segmentation and measurement of medical image using level set methods', *Magnetic Resonance Imaging*, 39, pp. 175–193, 2017.
- [25] Sharma, P., Singh, J.S.: 'A Novel Approach towards X-Ray Bone Image Segmentation using Discrete Step Algorithm', *International Journal of Emerging Trends & Technology in Computer Science (IJETTCS)*, 2(5), pp.191-195, 2013.
- [26] Harouni, A., Karargyris, A., Negahdar, M.: 'universal multi-modal deep network for classification and segmentation of medical images', 2018 IEEE 15th International Symposium on Biomedical Imaging (ISBI 2018), Washington, D.C., USA, pp. 872-876, 2018.
- [27] Saidy, L., Lee, C. C. : 'Chest X-Ray Image Segmentation Using Encoder Decoder Convolutional Network', 2018 IEEE International Conference on Consumer Electronics-Taiwan (ICCE-TW), Taichung, Taiwan, pp. 1-2, 2018.
- [28] Roy, P., Dutta, S., Dey, N., et al. : 'Adaptive thresholding: A comparative study', 2014 International Conference on Control, Instrumentation, Communication and Computational Technologies (ICCICT), Kanyakumari, India, pp.1320-1324, 2014.
- [29] N. Otsu, "A threshold selection method from gray-level histograms", *IEEE Transactions on Systems, Man, and Cybernetics*, 9 (1), pp. 62–66, 1979.
- [30] Dunik, J., Straka, O.: ' State estimate consistency monitoring in Gaussian filtering framework', *Signal Processing*, 148, pp. 145-156, , 2018.
- [31] Ito, K., Xiong, K.: 'Gaussian filters for nonlinear filtering problems', *IEEE Transactions on Automatic Control*, 45(5), pp. 910–927,2000.